A Novel Rat Model of Persistent Gouty Arthritis by Minimally Invasive Saturated Msu Embedding

Hanlin Xu
Huashan Hospital Fudan University
ShengKun Li
Fudan University
XiaoAo Xue
Fudan University
ZiYi Chen
Fudan University
Yinghui Hua (hua023@hotmail.com)
Department of Sports Medicine, Huashan Hospital, Fudan University. No.12 Urumqi Middle Rd., Shanghai 200040, China https://orcid.org/0000-0002-0767-1267

Research article

Keywords: Monosodium urate, intra-articular deposition, rat model, minimal invasive

Posted Date: September 18th, 2020

DOI: https://doi.org/10.21203/rs.3.rs-73068/v1

Abstract

Background: Animal models are valid for *in vivo* research on the pathophysiological process and drug screening of gout arthritis. Intra-articular injection of monosodium urate (MSU) is commonly used to establish animal model at present, while stable MSU deposition and tophi formation were rarely reported.

Method: A total of twenty-four rats were randomly allocated into six groups. Three intervention groups of rats received MSU embedment for 3-5 times, respectively. Sham groups received pseudo surgeries with normal saline (NS). Gross parameters and pathological features of synovium harvested from anterior capsule. Mechanical pain threshold tests of rats were conducted over a 96-hour period postoperatively.

Result: Significant synovial swelling was detected in the MSU group compared to the sham group($P<0.05$). Behavioral tests showed that the embedding of MSU resulted in prolonged mechanical hyperalgesia ($P<0.05$ during 2 hours to 96 hours postoperatively). MSU depositions enveloped by neutrophil extracellular traps (NETs) were detected where the IL-1β and TNF-α were co-expressed in embedding groups. Quantitative immunofluorescence suggested that the frequencies of MSU interventions promoted expression of proinflammatory factors ($P<0.05$).

Conclusion: A minimally invasive surgical method was developed to establish the novel rat model of intra-articular MSU deposition. This model was proved to be a simple reproducible method to mimic the pathological characteristics of intra-articular crystal arthritis.

Background

Gout is a systematic disease of uric acid disturbance with increasing incidence and burden of disease currently. [1–3] The central pathological mechanism of gout is the increased serum uric acid concentration exceeding the solubility threshold(6.8 mg/dL) and then crystals deposit in joint cavities.[3] Saturated urate undergoes a series of pathophysiological processes in the joint, including clustering, nucleation and growth in synovial fluid and deposited on surface of the articular cartilage, synovium or tendons. [4, 5]MSU crystal in synovial fluid induce inflammation characterized by the recruitment of neutrophils, expression of proinflammatory cytokine and the formation of NETs, which is considered as the typical structure of tophi including central MSU crystals enveloped densely by neutrophils. [6, 7] After repeated flares, the inflammatory response gradually erode the synovium and cartilage, resulting in joint pain and impaired function .[8]

Previous animal models of gout are mainly classified into hyperuricemia model, local injection model and gene knockout model.[9, 10] Injecting MSU suspension intra-articular or subcutaneous models were established to mimic the pathophysiological changes during gout flares for observing local inflammatory respons.[11–14] However, uricase is present in most common mammal experimental animals including rats, mice or rabbits, which metabolize and excrete urates rapidly. Hence, past models are designed for measuring the acute inflammatory response induced by MSU and the anti-inflammatory drug screening,

and manifested microscopic pathologically as synovial cell hyperplasia and acute inflammatory cell infiltration.[11, 15, 16]

To complement animal models for *in vivo* research of gouty arthritis, the present study performed accurate repeatable implantation of larger doses of MSU into the articular cavity and maintains a continuous high concentration of MSU in the articular cavity to resist the effect of uric acid oxidase. We assumed that multiple high-dose MSU implants would achieve optimal results, since sufficient MSU could counteract the decomposition by uricase and the interventions simulate the pathophysiological process of crystal deposition caused by recurrent gout flares.

In summary, the purpose of this article is to introduce a novel rat model of persistent gout arthritis characterized by MSU deposition in pathological sections and more severe joint swelling and pain. We hope to provide a producible, economical, and accurate in vivo method for studies on the deposition and erosion of MSU or influence of various factors on this process in future.

Methods

Animal study

A total of twenty-four male SD rats aged 8 weeks and weighted from 160 to 180 grams were purchased from Shanghai Lab. Animal Research Center. Experimental procedures passed a review by the Animal Welfare and Ethics Group, Department of Experimental Animal Science; Shanghai Medical College of Fudan University, Shanghai, China (Approval Number:2019020405). The MSU crystal was prepared by PH titration of 99% uric acid (Sigma, USA) according to the method proposed by previous study.[12] A MSU crystal suspension of 100 mg/ml was prepared then. All the rats were randomly separated into four groups. MSU suspension was embedded into joint cavity at 0.2 ml in MSU intervention groups respectively, while 0.2 ml NS was injected into the joint cavity in sham groups. Minimally invasive procedures were performed three to five times for each rat, depending on the group, and the intervals between operations were five days. (Fig. 1)

The animals were housed in plastic cages in a 12-hour light and dark cycle with free access to food and water. Anesthesia was induced by inhaling 3% isoflurane and maintained by inhaling 1.5% isoflurane. Bilateral knee joints of each rat were operated under anesthesia. An 8 mm incision was made on the lateral side of the joints. The joint capsule was incised longitudinally lateral to patellar tendon to expose the femoral trochlear. A chondral defect was drilled by kirschner wire (1.5 mm in diameter, 2 mm in depth) in the femoral trochlear groove. After the crystal is accurately embedded in the joint, all incisions were cleaned and sutured after surgeries and there were no restrictions on animal activities (Fig. 2).

The dose and the test period are determined based on the preliminary experiments. Longer intervention interval could lead to poor deposition effect, while shorter intervention intervals is detrimental to animals' recovery and welfare. The 5-day interval ensures the healing of the incision. The experimental results also showed that the activity and 50%PWT of the sham group recovered normal 5 days after surgeries.

Gross measurement

Rats were sacrificed by cervical dislocation on the five days after the last surgery. The synovium of joint cavity was dissected and harvested for further analysis. The width of the patellar ligament and the thickness of the synovium were measured by micrometer caliper (I. QUIP, China) to evaluate effects of MSU on local tissues. Anterolateral synovium (5mm × 5 mm) on the lateral side of the patellar tendon is harvested, and the area of incisions and sutures is avoided. The area below the patella is used as the patellar tendon sampling area (10mm × 3 mm). Each specimen will be measured three times and averaged as the final result. All gross measurements are performed and recorded by a blinded researcher.

Histologic Examination

Unless particularly stated, reagents were purchased from Sigma Chemical Co.St.Louis, MO, USA and Servicebio, Wuhan, China.The tissues were fixed in 4% paraformaldehyde. Dehydration was processed and embedded in paraffin. The synovium rats were processed for H&E staining and immunofluorescence staining as previous described.[17] For immunofluorescent staining, the synovium specimens were stained for IL-1β (ProteinTech, 16806-1-AP), TNF-α (ProteinTech, 60291-1-lg). Ortho-Fluorescent microscope (Nikon, Japan) and image system (Nikon, Japan) were used for imaging of samples.

For quantitative analysis, Image-pro Plus 6.0 software (Media Cybernetics, Inc., Rockville, MD, USA) was used to convert green/red fluorescence monochrome photos into black and white images, and then the unified standard for judging all positive photos was determined. The integral optical density (IOD) and pixel AREA of tissues of positive images were obtained by analyzing each photo. Average optical (AO) density value was calculated, and AO = IOD/AREA. The higher the AO value indicated the higher the positive expression level.

Behavioral tests

The mechanical allodynia was determined using a series of calibrated von Frey filaments (North Coast, USA). Fifteen minutes before the test, the rats were individually habituated in a transparent plexiglass chamber on an elevated mesh floor. The filaments were applied perpendicularly to plantar surface of the hind paw until the filaments buckled slightly for 3 seconds. A sharply withdrawal of the paw and licking in response to the application or removal of stimulation were considered as positive response.[15, 16] The paw withdrawal threshold (PWT) was determined using the Up-and-Down Method as described in previous studies.[18]

After measuring the baseline(6.33±1.58 g) in the preliminary experiment, the fiber filaments of 4 grams were selected as the first stimulus. In formal trials, rats that did not respond to filaments of 16 grams or more were excluded. This is because when the filaments stimulated more than 10% of the rats' body weight, the stimulation was more like lifting the hindfoot than stinging it. All behavior tests are performed and recorded by independent researcher and the interventions on rats was blind to her.

Statistical Analysis

Statistical analyses were performed by GraphPad Prism 8.0.1 software. All datasets were tested for normality for t-test, and if the normality test failed, the Mann Whitney rank-sum test was used for intra-group comparison. Results are expressed as mean ± SD. P value < 0.05 is considered as significant.

Result

All the rats received surgical interventions according to the experimental protocols. No incision-related infection, MSU leakage or other complications occurred.

Gross measurements and behavioral tests were conducted to evaluate the local effects of MSU-mediated inflammation. Significant synovial swelling was detected in the MSU group compared to the sham group five days after the last intervention ($P = 0.0250$ after three interventions, $P < 0.0001$ after four or five interventions) (Fig. 3a), while patellar ligament was not affected by MSU inflammation($p > 0.05$ in all groups) (Fig. 3b).

Behavior tests revealed abnormal reductions of the PWT in MSU groups compared to the sham groups started with2 hours after the intervention ($p < 0.05$). Within 24 to 48 hours after the operation, the pain threshold of the rats in the sham groups gradually returned to the normal level. The pain threshold of the MSU groups also recovered, but it was significantly lower than that in the sham group within 96 hours ($p < 0.05$ during 2 hours to 96 hours postoperatively) (Fig. 3c). Notably, this reduction in pain threshold was shown to be related not to the frequencies of operations (Fig. 3d), but to whether MSU was embedded.

The histopathological differences between the MSU group and the sham group were demonstrated by H&E staining. Inflammatory cell infiltrations in the synovium and aligned collagenous fibers in the saline groups. In MSU intervention group, the sections from showed serious synovial hyperplasia, cell proliferation, and collagen fiber disorder increased with the frequencies of interventions (Fig. 4a). Different from the previous acute gout arthritis model, recruited neutrophil packed with MSU crystal deposition was observed in MSU group. The H&E stain clearly demonstrates the eosinophilic acellular structure (MSU crystals) and multiple surrounding layers of lobulated neutrophils (Fig. 4b).

Immunofluorescence revealed the expression level of inflammatory factors in synovial tissue after MSU implantation. IL-1β and TNF-α are highly co-expressed in aggregated inflammatory cells (Fig. 5a). Further quantitative average optical (AO) analysis showed that the expression levels of two cytokines were up-regulated with the increase of intervention frequencies, which also demonstrated the typical MSU-mediated synovial inflammation *in vivo* (Fig. 5b).

Discussion

This study designed a reliable and economical animal model for persistent gout arthritis in relative short time, manifested by significantly prolonged gross and behavioral abnormalities, as well as intra-articular

MSU deposition and the tophi formation. This research may attract broad interest for researchers focusing on a various of crystalline arthritis.

Animal models of gout are necessary basis for researchers to understand the disease progress and to determine potential treatments and prevention measures. A literature search based on PubMed database was conducted among studies of gouty arthritis over the past decade, more than 120 articles applied model mentioned above to study the pathophysiological mechanism and therapies efficacy. However, due to the lack of appropriate animal models, limited studies are available regarding the formation, growth, attachment and deposition of MSU *in vivo*,[19] which leaves a research gap in the study of the continuous interaction of crystals within the tissues *in vivo*.

Intra-articular injection of MSU is an optimal model for acute inflammation, while no report of chronic pathological changes is reported in injection models.[12, 20] Active uric acid oxidase is lost in human but presenting in most mammals (such as rats, rabbits, etc.), which causes that serum uric acid levels of other mammals are only one-tenth of human. [21, 22] Hence, limited dose of MSU injection often cause acute joint inflammation, but the threshold of tophi formation and crystal deposition are rarely reached. Wu et.al introduced a method of homologous recombination in mice embryonic stem cells to establish a mice model lacking urate oxidase.[23] Congenital MSU deposition in kidney were observed in mutated mice, but the mortality rate exceeded 50 percent in the first four weeks after birth. Due to the low survival rate, the difficulty of gene editing and cost of experiment, it is hard to be comprehensively applied for further studies. Other researchers performed intraperitoneal or subcutaneous injection of MSU to simulate gout synovitis and have achieved good results, but this air-pouched method is not suitable for the study of chronic gouty arthritis focusing the changes of synovial membrane, cartilage and bone[24–26]

The present study puts accurate repeatable implantation of larger doses of MSU into the articular cavity and maintains a continuous high concentration of MSU in the articular cavity to resist the effect of uric acid oxidase. Pain and joint swelling are typical symptoms of gout arthritis. In injection model, local symptoms are proved to present as self-limiting and relive within 72 hours.[16] Consistently, The reduction of the PWT in MSU injection models was reported maintained within 48 to 72 hours in previous researches.[16] In contrast, this study significantly prolonged the persistence of local symptoms, with significant synovial swelling and mechanical hyperalgesia more than five days after interventions. This outcome is caused by MSU embedding rather than surgical incision due to the presence of a control group. In terms of pathology, MSU crystal deposition was observed surrounded by IL -1β, TNF -α positive inflammatory cell. This is the first report of exogenous MSU deposition in synovium in animal models into, providing potential tools for clinical identification and debridement. The model also provides an ideal approach for further studying the pathophysiological changes of MSU deposition *in vivo* and accurate removal of MSU deposition in tissue.

Compared with the injection modeling method, more persistent joint inflammation and crystal deposition are observed in this study for three main reasons, including higher dose, more accurate implantation, and combination with artificial defect. 1) The implantation dose was significantly more sufficient than the

traditional injection method. Injection dose distributed between 0.5 mg to 5.0 mg in previous research,[12, 15, 16, 27] while the total embedding dose of MSU in this experiment reached 60 to 100 mg. High-dose MSU intervention, though larger than other injection models, was shown to be safe and no lesions or symptoms outside the joint was found. The results proved that MSU crystals were deposited in the synovium by inflammatory cells before being decomposed by uricase. 2) The space of rats' knee articular cavity is limited with multiple contents including ligaments, cartilage, and meniscus. In addition, saturated MSU crystals tend to precipitate at room temperature and then block injection needles. Swell and effusion of tissues induced by MSU could further aggravate the stenosis of cavity and increase the failure rate of repeated injection. Minimally invasive approach solved this problem by exposing the joint cavity and locating position of MSU crystals accurately. 3) Previous studies suggested that physic impact would result in traumatic arthritis in rabbits.[28, 29] A radiographic study also found a strong relationship between bone erosion and tophi formation.[30] Therefore, impaired cartilage accelerate the establishment of gouty arthritis model and then shorten the trial period. [31]

There are some limitations in the present study as the following: 1) The procedures of this minimally invasive operation required practice and repetition in order to get a satisfied result of MSU embedding. Basic surgical training is required to meet the operational requirements. 2) The duration of this model was still much less than the natural course of chronic gouty arthritis in human which lasting for a few years. Further studies have to include a more convenient way to embed MSU and increase the sessions of embedment to extend the affect time. It is not verified how long the model will last without MSU embedding, which will be one of the research directions in the future. 3) In this study, synovial crystal deposition was observed, but tendon, ligament, cartilage, or bone was not involved. Due to the process of sections decalcification, some technical difficulties of preserving crystals from strong acid need to be overcome. Sections of osteochondral specimens should also be analyzed in further researches.

Conclusion

A minimally invasive surgical method was developed to establish the novel rat model of chronic gouty arthritis. This model was proved to be a simple repeatable method and to mimic the pathological characteristics of human persistent gouty arthritis.

Abbreviations

AO	average optical
IOD	integral optical density
MSU	monosodium urate
PWT	paw withdrawal threshold

Declarations

Ethics approval and consent to participate

Experimental procedures passed a review by the Animal Welfare and Ethics Group, Department of Experimental Animal Science; Shanghai Medical College of Fudan University, Shanghai, China (Approval Number:2019020405).

Consent for publication

Not applicable.

Availability of data and materials

The datasets used and/or analysed during the current study are available from the corresponding author on reasonable request.

Competing interests

The authors declare that they have no competing interests.

Funding

We thank the financial support from the Shanghai Municipal Science and Technology Project (ID: 17441900900) in process of collection, analysis, and interpretation of data.

Authors' contributions

Y.H designed and directed the study. H.X and S.L performed animal surgical procedure. Z.C carried out behavior tests. H.X, A.X and Z.C collected and analyzed data, respectively. Y.H, H.X and A.X wrote the manuscript with contributions from all the authors.

Acknowledgements

Not applicable.

References

1. Roddy E, Choi HK. Epidemiology of gout. Rheum Dis Clin North Am. 2014;40(2):155–75.
2. Mikuls TR, Farrar JT, Bilker WB, Fernandes S, Schumacher HR Jr, Saag KG. Gout epidemiology: results from the UK General Practice Research Database, 1990–1999. Ann Rheum Dis. 2005;64(2):267–72.
3. Ragab G, Elshahaly M, Bardin T. Gout: An old disease in new perspective - A review. J Adv Res. 2017;8(5):495–511.
4. O'Connor PJ. Crystal deposition disease and psoriatic arthritis. Semin Musculoskelet Radiol. 2013;17(1):74–9.

5. Schlesinger N. Management of acute and chronic gouty arthritis: present state-of-the-art. Drugs. 2004;64(21):2399–416.
6. Schett G, Schauer C, Hoffmann M, Herrmann M. Why does the gout attack stop? A roadmap for the immune pathogenesis of gout. RMD Open. 2015;1(Suppl 1):e000046.
7. Schauer C, Janko C, Munoz LE, Zhao Y, Kienhofer D, Frey B, Lell M, Manger B, Rech J, Naschberger E, et al. Aggregated neutrophil extracellular traps limit inflammation by degrading cytokines and chemokines. Nat Med. 2014;20(5):511–7.
8. Schlesinger N, Thiele RG. The pathogenesis of bone erosions in gouty arthritis. Ann Rheum Dis. 2010;69(11):1907–12.
9. Liu Z, Chen T, Niu H, Ren W, Li X, Cui L, Li C. The Establishment and Characteristics of Rat Model of Atherosclerosis Induced by Hyperuricemia. Stem Cells Int. 2016;2016:1365257.
10. Bluestone R, Waisman J, Klinenberg JR. Chronic experimental hyperuricemic nephropathy. Lab Invest. 1975;33(3):273–9.
11. Pineda C, Fuentes-Gomez AJ, Hernandez-Diaz C, Zamudio-Cuevas Y, Fernandez-Torres J, Lopez-Macay A, Alba-Sanchez I, Camacho-Galindo J, Ventura L, Gomez-Quiroz LE, et al. Animal model of acute gout reproduces the inflammatory and ultrasonographic joint changes of human gout. Arthritis Res Ther. 2015;17:37.
12. Coderre TJ, Wall PD. Ankle joint urate arthritis (AJUA) in rats: an alternative animal model of arthritis to that produced by Freund's adjuvant. Pain. 1987;28(3):379–93.
13. Hu Y, Yang Q, Gao Y, Guo X, Liu Y, Li C, Du Y, Gao L, Sun D, Zhu C, et al: **Better understanding of acute gouty attack using CT perfusion in a rabbit model**. *Eur Radiol* 2018.
14. McCarty DJ Jr, Phelps P, Pyenson J. Crystal-induced inflammation in canine joints. I. An experimental model with quantification of the host response. J Exp Med. 1966;124(1):99–114.
15. Marcotti A, Miralles A, Dominguez E, Pascual E, Gomis A, Belmonte C, de la Pena E. Joint nociceptor nerve activity and pain in an animal model of acute gout and its modulation by intra-articular hyaluronan. Pain. 2018;159(4):739–48.
16. Chai W, Tai Y, Shao X, Liang Y, Zheng GQ, Wang P, Fang J, Liu B. Electroacupuncture Alleviates Pain Responses and Inflammation in a Rat Model of Acute Gout Arthritis. Evid Based Complement Alternat Med. 2018;2018:2598975.
17. Al-Madol MA, Shaqura M, John T, Likar R, Ebied RS, Schäfer M, Mousa SA. Comparative Expression Analyses of Pro- versus Anti-Inflammatory Mediators within Synovium of Patients with Joint Trauma, Osteoarthritis, and Rheumatoid Arthritis. Mediators Inflamm. 2017;2017:1–11.
18. Dixon WJ. The Up-and-Down Method for Small Samples. Publications of the American Statistical Association. 1965;60(312):967.
19. Chhana A, Lee G, Dalbeth N. Factors influencing the crystallization of monosodium urate: a systematic literature review. BMC Musculoskelet Disord. 2015;16:296.

20. Kang L, Miao MS, Liu HJ, Li N. [Analysis of animal models based on clinical symptoms of gout]. Zhongguo Zhong Yao Za Zhi. 2018;43(22):4547–52.
21. Wu XW, Muzny DM, Lee CC, Caskey CT. Two independent mutational events in the loss of urate oxidase during hominoid evolution. J Mol Evol. 1992;34(1):78–84.
22. Friedman TB, Polanco GE, Appold JC, Mayle JE. On the loss of uricolytic activity during primate evolution–I. Silencing of urate oxidase in a hominoid ancestor. Comp Biochem Physiol B. 1985;81(3):653–9.
23. Wu X, Wakamiya M, Vaishnav S, Geske R, Montgomery C Jr, Jones P, Bradley A, Caskey CT. Hyperuricemia and urate nephropathy in urate oxidase-deficient mice. Proc Natl Acad Sci U S A. 1994;91(2):742–6.
24. Ryckman C, McColl SR, Vandal K, de Medicis R, Lussier A, Poubelle PE, Tessier PA. Role of S100A8 and S100A9 in neutrophil recruitment in response to monosodium urate monohydrate crystals in the air-pouch model of acute gouty arthritis. Arthritis Rheum. 2003;48(8):2310–20.
25. Martin WJ, Shaw O, Liu X, Steiger S, Harper JL. Monosodium urate monohydrate crystal-recruited noninflammatory monocytes differentiate into M1-like proinflammatory macrophages in a peritoneal murine model of gout. Arthritis Rheum. 2011;63(5):1322–32.
26. Rull M, Clayburne G, Sieck M, Schumacher HR. Intra-articular corticosteroid preparations: different characteristics and their effect during inflammation induced by monosodium urate crystals in the rat subcutaneous air pouch. Rheumatology. 2003;42(9):1093–100.
27. dos Santos RM, Oliveira SM, Silva CR, Hoffmeister C, Ferreira J, Assreuy J. Anti-nociceptive and anti-edematogenic effects of glibenclamide in a model of acute gouty attack in rats. Inflamm Res. 2013;62(6):617–25.
28. Milentijevic D, Rubel IF, Liew AS, Helfet DL, Torzilli PA. An in vivo rabbit model for cartilage trauma: a preliminary study of the influence of impact stress magnitude on chondrocyte death and matrix damage. J Orthop Trauma. 2005;19(7):466–73.
29. Fening SD, Jones MH, Moutzouros V, Downs B, Miniaci A. Method for Delivering a Controlled Impact to Articular Cartilage in the Rabbit Knee. Cartilage. 2010;1(3):211–6.
30. Dalbeth N, Clark B, Gregory K, Gamble G, Sheehan T, Doyle A, McQueen FM. Mechanisms of bone erosion in gout: a quantitative analysis using plain radiography and computed tomography. Ann Rheum Dis. 2009;68(8):1290–5.
31. Kuo CF, Grainge MJ, Zhang W, Doherty M. Global epidemiology of gout: prevalence, incidence and risk factors. Nat Rev Rheumatol. 2015;11(11):649–62.

Figures

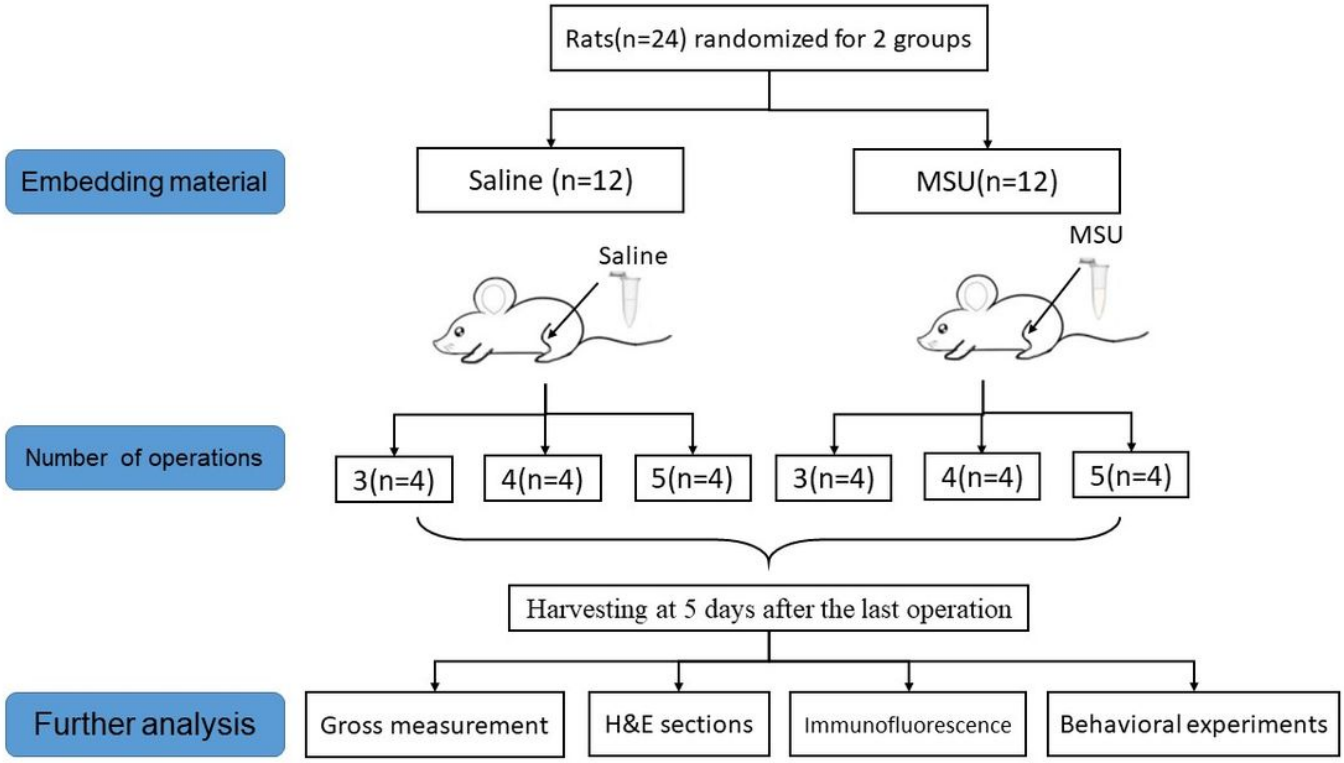

Figure 1

Flow diagram of animal study.

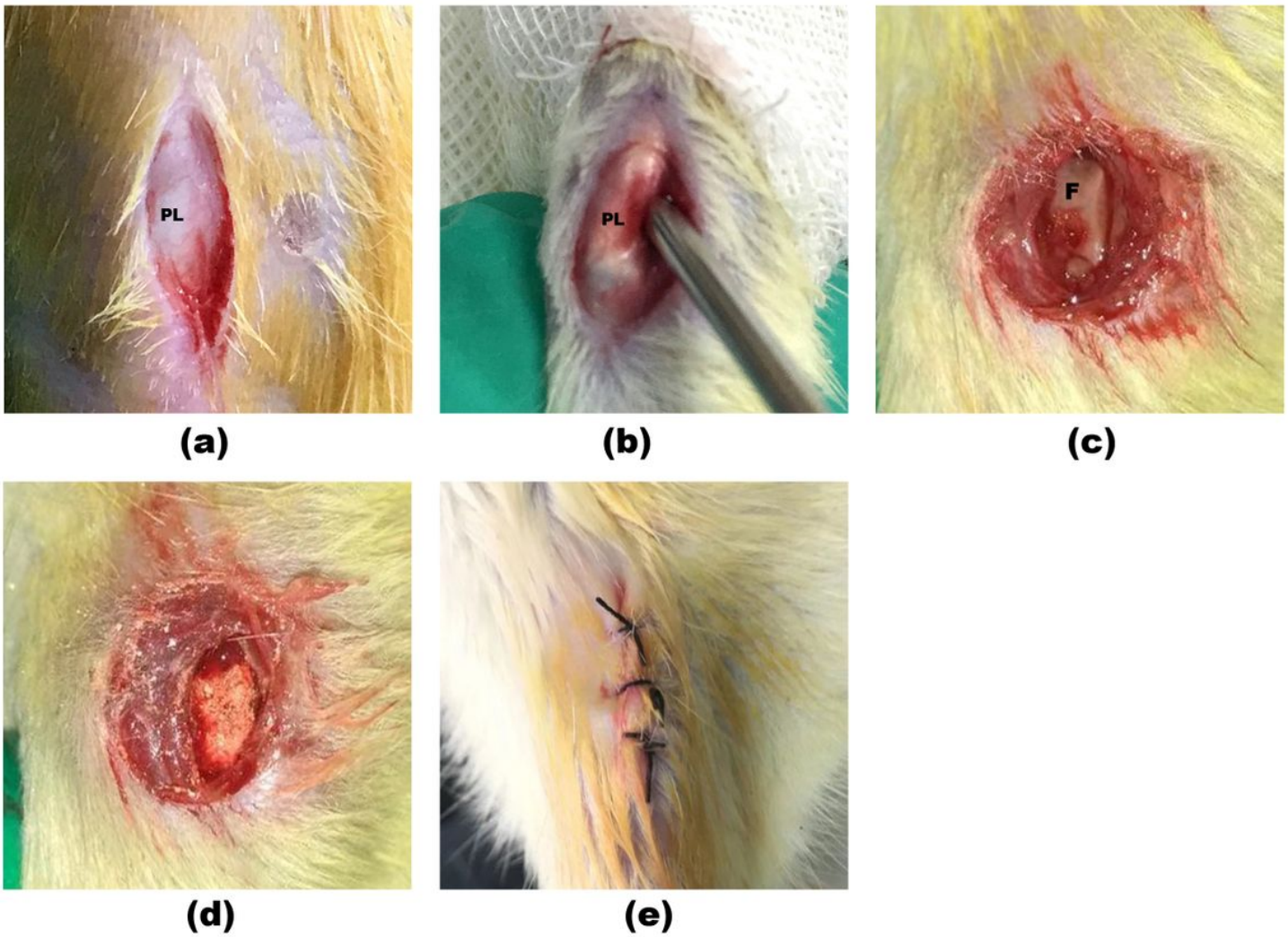

Figure 2

Operating procedures of MSU embedment on rats. Protocol for establishing MSU embedment models. (a-b) The skin and capsule of the joint was incised layer by layer along the lateral side of the patellar ligament, and joint cavity of the knee was exposed. (c) The intercondylar fossa cartilage of femur was damaged by kirschner wire. (d) The MSU crystal was embedded. (e) The incisions of articular capsule and skin were closed. PL：Patellar Ligament F: Femur

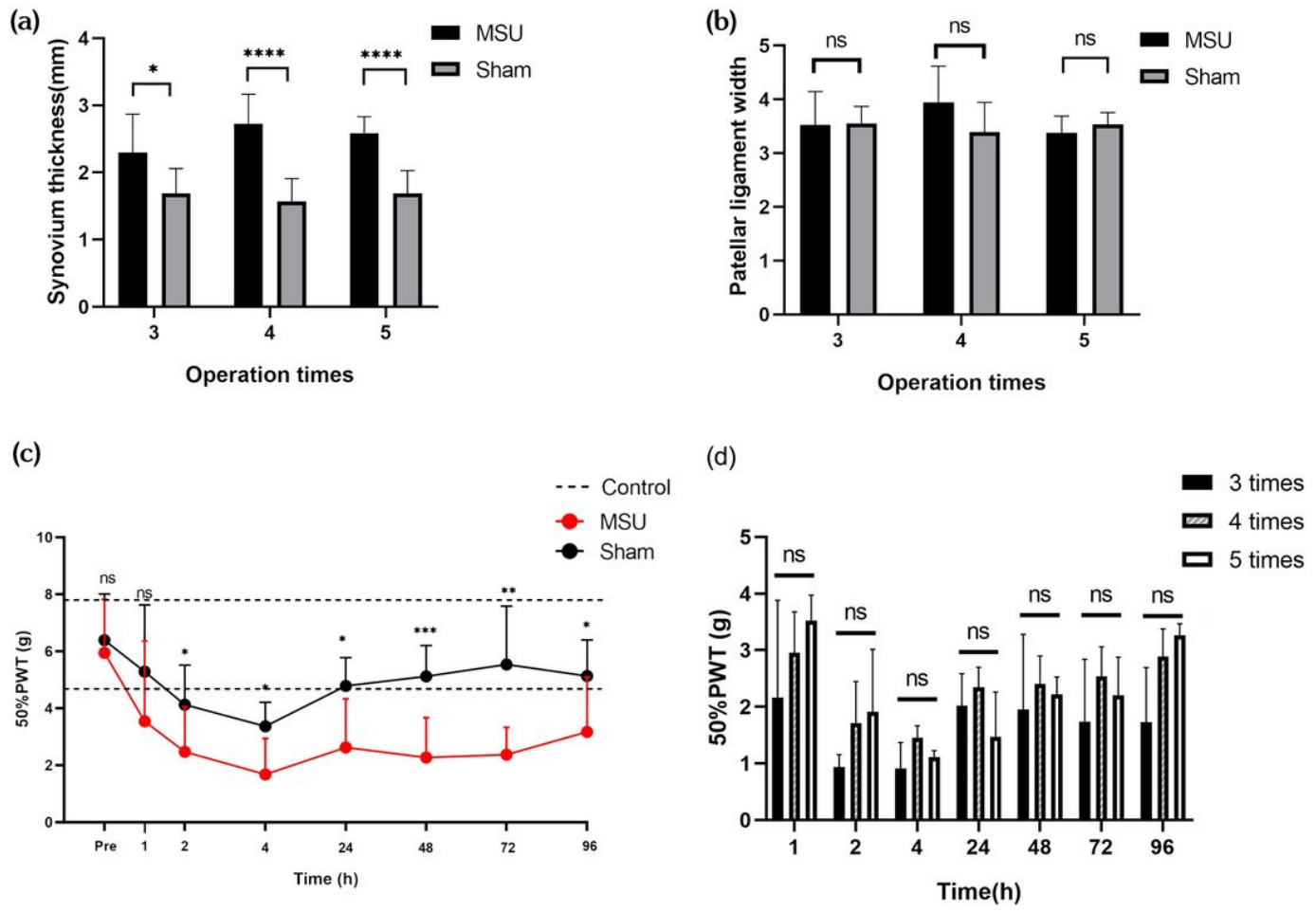

Figure 3

Gross changes in joint tissue and mechanical pain threshold in rats after MSU embedding. (a) The thickness of the synovium lateral to the patellar ligament in the rats. The synovium thickness of the MSU groups were greater than that of sham groups. (n=8 for each group; two-tailed t-test, *P =0.0250, ****P <0.0001). (b) No significant (NS) differences was detected between sham groups and MSU groups (n=8 for each group; two-tailed t-test). (C) The 50%PWT of the wild-type littermates(n=8) is shown between the dotted lines(6.33±1.58g). As a result of the operation, rats in all groups were more sensitive to the stimulation of Von Frey filaments within 24 hours after the operation, showing a decrease in mechanic pain threshold. In the sham group, the pain threshold returned to nearly normal level till 24 to 48 hours after operations. However, in MSU group, on the other hand, continued PWT reduction was detected within 3 to 4 days after surgeries. (n=7 for sham group; n=10 for MSU group; two-tailed Mann Whitney test was applied in time point of 4 hours and 24hours; two-tailed t-test was applied for other time points; Pre: P>0.05, 1 hour: P>0.05; 2 hours: P= 0.0461;4 hours: P= 0.0164; 24 hours: P= 0.0311; 48 hours: P= 0.0005; 72 hours: P= 0.0010; 96 hours: P= 0.0355) (D) No significant differences was detected between MSU groups with different operation frequencies at all time points. (n=4 for each group; One-way ANOVA

was applied for each time point, P>0.05 at all time points with different operation frequencies) The x axis represents time points pre and after operations. Data shown as mean ± s.e.m.

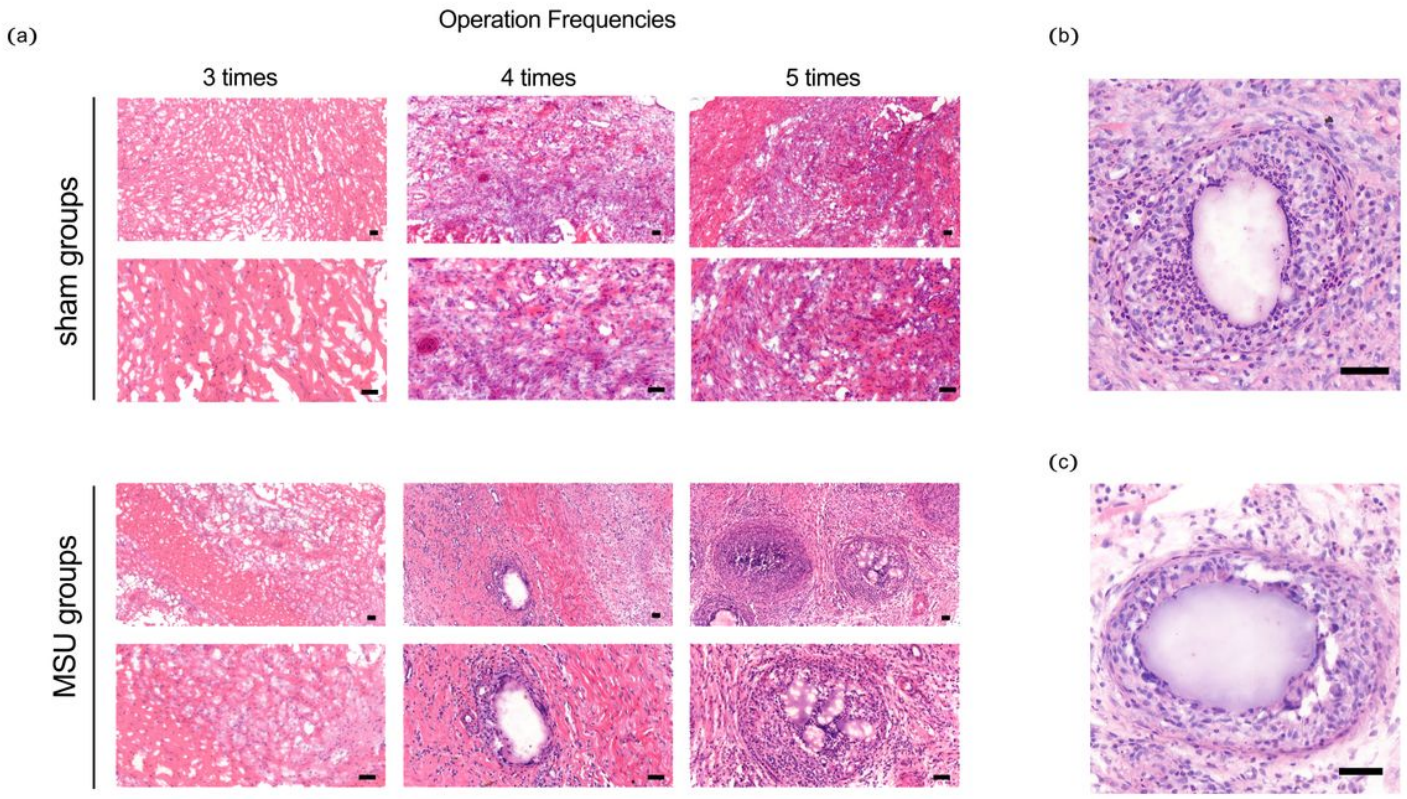

Figure 4

Inflammatory cells infiltration and deposition of MSU in synovial tissue. Representative images of pathological section showed a progressive MSU - mediated inflammation. (a) Top, in the sham groups, the synovial inflammation as well as disordered collagenous fibers were observed. Three below columns, with the increase of embedding times and the extension of time, MSU deposited in tissues mediating the immune response and recruiting a large number of inflammatory cells. MSU deposition were surrounded by the collagen fibers (outer layer) and the inflammatory cells (inner layer). (b-c) Representative images of MSU deposition surrounded by inflammatory cells. Deposition of MSU was mainly surrounded by lobulated neutrophils with monocytes and lymphocytes in the outer layer. Scale bars, 50 μm.

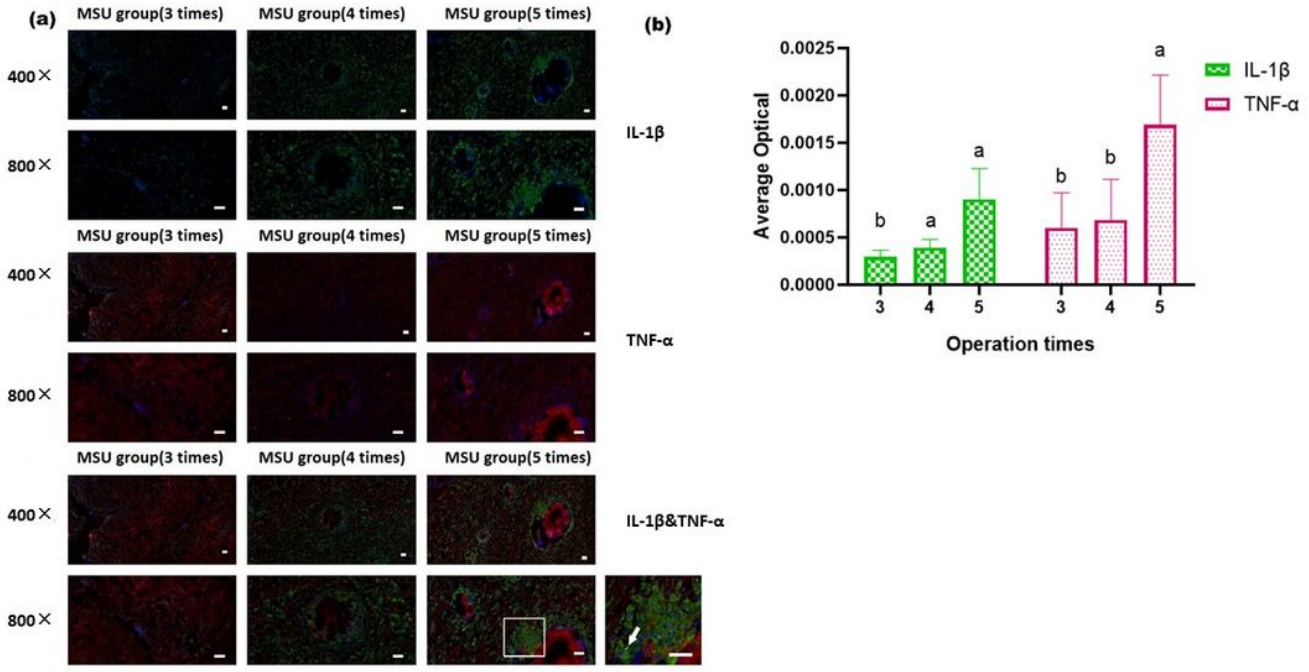

Figure 5

Immunofluorescence revealed upregulation of IL-1β expression in the MSU embedding rat model. (a)Representative images of immunofluorescence showed regulation of cytokines expression in MSU embedding groups. IL-1β(green) expression was significantly upregulated in tissues. Similarly, TNF-α(red) is also highly expressed around MSU deposition. Arrow indicated a significant expression of IL-1β in cells surrounding MSU. (b) Further quantitative average optical (AO) analysis showed that the expression levels of two cytokines were up-regulated with the increase of intervention frequencies. (n=4 for each group; One-way ANOVA and Tukey's multiple comparisons tests were applied for each cytokine.) Scale bars, 50 μm.

Supplementary Files

This is a list of supplementary files associated with this preprint. Click to download.

- AuthorChecklistE10only.pdf